

Fabrication of MgO-coated TiO₂ nanotubes and application to dye-sensitized solar cells

Hun Park · Dae-Jin Yang · Ho-Gi Kim · Seong-Je Cho ·
Su-Chul Yang · Hyunjung Lee · Won-Youl Choi

Received: 31 May 2007 / Accepted: 2 October 2007 / Published online: 19 October 2007
© Springer Science + Business Media, LLC 2007

Abstract Dye-sensitized solar cells (DSCs) are more spotlighted than conventional photovoltaic devices due to their relatively low cost, easy fabrication and high efficiency. However, there are limitations to increase the conversion efficiency of DSCs. The limiting factors are the quantity of dye adsorption and charge recombination between TiO₂ electrode and electrolyte. Coating other materials such as high energy band gap insulators or semiconductors on the TiO₂ electrode enhances dye adsorption and reduces charge recombination. We fabricated DSCs based on bare TiO₂ nanotube arrays and 0.02 and 0.04 M MgO coated TiO₂ nanotube arrays. MgO layer increased the photovoltage and photocurrent. The overall conversion efficiency of DSCs using 0.02 M MgO coated TiO₂ nanotubes was 1.61%. MgO formed insulating layers between TiO₂ nanotube array electrode and electrolyte. Charge recombination was inhibited at the interfaces of TiO₂ nanotube array electrode and electrolyte by MgO insulating layers. MgO coating also

improved dye adsorption because iso-electric point (IEP) of MgO was larger than TiO₂. When the IEP of coating material is larger than TiO₂, the chemical attraction between the electrode surface and Ru-based dye molecule is increased.

Keywords TiO₂ · Nanotube · Anodic oxidation · Dye-sensitized solar cells · MgO

1 Introduction

Dye-sensitized solar cells based on nanocrystalline TiO₂ photoelectrode are of great interest as an alternative to the conventional silicon solar cells because of their high performance and low-cost production [1, 2]. In randomly packed TiO₂ nanocrystalline films, it has been mentioned that electron transport is limited by the residence time of electrons in traps [3] and structural disorder at the contact between two crystalline nanoparticles, resulting in low efficiency of collecting the injected electrons [4]. Recently, TiO₂ nanotube structures have received considerable attention to an application in photocatalysis, sensing, photoelectrolysis and photovoltaics [5]. In application to DSCs, vertically oriented TiO₂ nanotube arrays have higher charge collection efficiencies than a nanoparticle-based structure due to their faster transport and slower recombination of electrons [6, 7]. On the other hand, coating surface of the nanocrystalline photoelectrode with a high energy band-gap material has received much attention for enhancing the photovoltaic performance [8, 9]. These coating layers retards back transfer of electrons to the electrolyte and minimize charge recombination [8–12]. Moreover, dye attachment becomes more favorable because the surface of coating material is more basic than TiO₂, and consequently, a light harvesting efficiency can be increased [8–10].

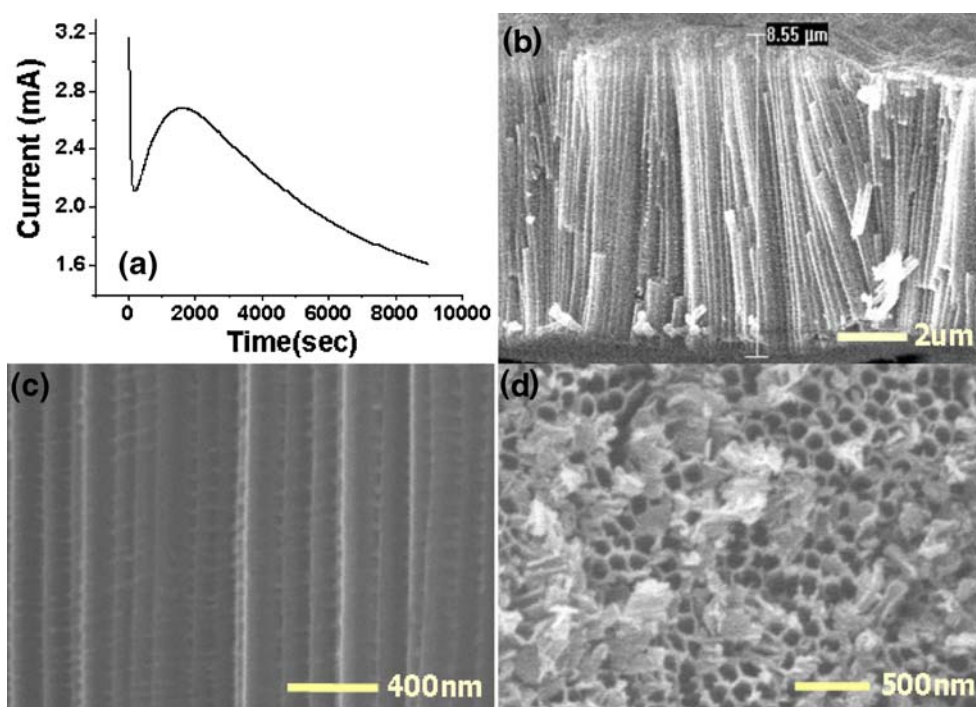
H. Park · D.-J. Yang · H.-G. Kim
Department of Materials Science and Engineering,
Korea Advanced Institute of Science and Technology,
Daejeon 305-701, South Korea

S.-J. Cho
Research center, BioAlpha Inc.,
Seongnam 462-120, South Korea

S.-C. Yang · H. Lee
Hybrid Research Center,
Korea Institute of Science and Technology,
P.O. Box 131,
Seoul, South Korea

W.-Y. Choi (✉)
Department of Metal and Materials Engineering,
Kangnung National University,
Kangnung 210-702, South Korea
e-mail: cwiy@kangnung.ac.kr

Fig. 1 Formation of TiO₂ nanotube arrays by anodic oxidation process at a constant voltage 60 V in 0.25wt.% NH₄F contained ethylene glycol solution kept at 30 °C for 3 h (a) current transient curve in anodization process (b) cross section image of 8.55 μm thickness TiO₂ nanotube arrays (c) magnified image of (b) (d) top surface image of TiO₂ nanotube arrays



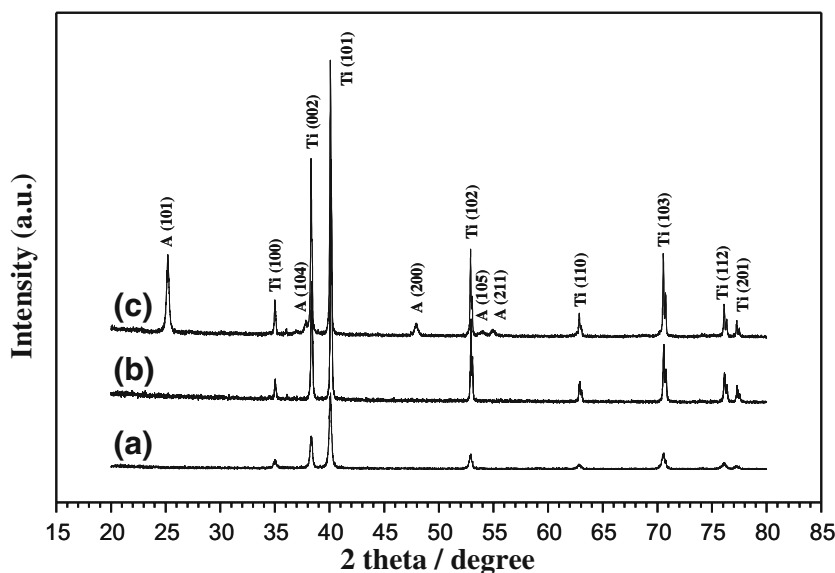
Reduced charge recombination and increased amount of dye adsorption are expected to give a higher conversion efficiency of DSCs. In this study, DSCs was fabricated using anodized TiO₂ nanotube array and the solar cell performance was evaluated. To increase the efficiency, MgO layer having high energy band-gap was coated on TiO₂ nanotube array.

2 Experimental

Highly ordered TiO₂ nanotube arrays were grown by anodic oxidation of 1 mm thick titanium bulk metal at a constant potential 60 V (ramping up to 60 V with 0.1 V/s) in the

ethylene glycol solution containing 0.25 wt.% NH₄F kept at 30 °C for 3 h. The anodized samples were annealed at 500 °C for 30 min to induce anatase phase of the initially formed amorphous TiO₂ nanotube arrays. X-ray diffraction (XRD) analysis was done before and after annealing to confirm the crystallinity of the TiO₂ nanotubes. The crystalline structures of the materials were determined by X-ray diffractometry (Rigaku D/MAX-RC) excited with CuK_α radiation. The samples were immersed in 0.02 and 0.04 M Mg(CH₃COO)₂·4H₂O aqueous solution kept at 65 °C for 30 min to form Mg(OH)₂ layers on TiO₂ nanotube arrays. To fill the TiO₂ nanotubes with the solution, the samples were vacuumed during immersing. The immersed samples were rinsed with deionized

Fig. 2 XRD analysis data of (a) Ti bulk metal, (b) as-anodized TiO₂ nanotubes and (c) annealed TiO₂ nanotubes



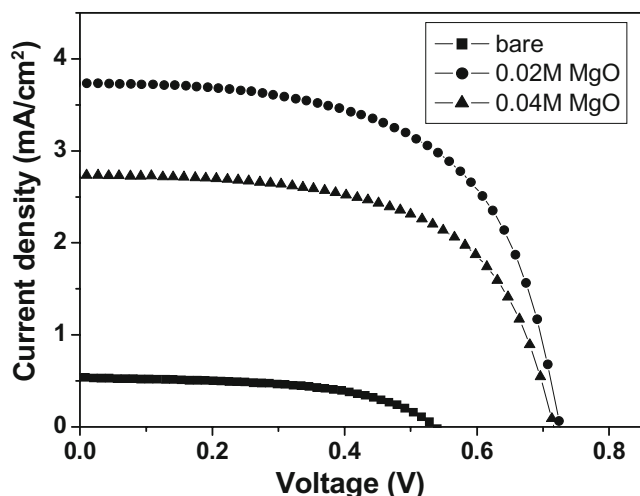


Fig. 3 Current–voltage characteristics under AM 1.5 illumination for DSCs based on bare TiO₂, 0.02 M MgO coated TiO₂ and 0.04 M MgO coated TiO₂ nanotube arrays

water. These coated samples were annealed at 450 °C for 10 min to convert Mg(OH)₂ to MgO [13].

TiO₂ nanotube photoelectrodes with and without MgO layer were immersed for ~1 day in an ethanol solution containing 3×10^{-4} M of N719 dye. The dye-adsorbed photoelectrodes were rinsed with ethanol and dried at room temperature. The liquid electrolytes consisted of 0.6 M 1-hexyl-2,3-dimethyl-imidazolium iodide (C6DMI), 0.05 M iodine (I₂), 0.1 M lithium iodide (LiI) and 0.5 M 4-tert-butylpyridine in 3-methoxypropionitrile. Pt counter electrode was prepared by spin-coating H₂PtCl₆ solution (7 mM in isopropyl alcohol) onto the FTO glass; this was then sintered at 450 °C for 30 min. The electrode of TiO₂ nanotube arrays and the counter electrode were spaced and sealed by 60 μm thick hot melt film as a spacer. Photocurrent–voltage characteristics (J–V curves) were measured under AM 1.5 illumination (Keithley Model 2400 source measure unit). A 1,000 W xenon lamp (Oriel, 91193) was used as a light source.

3 Results and discussion

The formation of nanotube arrays in electrolytic solution is the result of three simultaneously occurring process: (1) field assisted oxidation of Ti metal to form TiO₂, (2) field assisted dissolution of Ti metal ions in the electrolyte, and (3) chemical dissolution of Ti and TiO₂ due to etching by fluoride ions [14, 15]. In real time potentiostatic anodization behavior of Ti metal, initial current between cathode and anode decreased due to the formation of TiO₂ layers on Ti bulk metal, as shown in Fig. 1. When the TiO₂ layers were etched by fluoride ions and Ti metal was exposed, the generated currents increased to some extent. As the surface of the exposed Ti metal was converted into TiO₂ layer, the

Table 1 Performances of DSCs based on bare TiO₂, 0.02 M MgO coated TiO₂, and 0.04 M MgO coated TiO₂ nanotube arrays.

MgO coating	V_{oc} (v)	J_{sc} (mA/cm ²)	FF (%)	η (%)
Bare	0.5370	0.535	54.23	0.16
0.02 M	0.7254	3.732	59.58	1.61
0.04 M	0.7157	2.738	59.98	1.18

currents decreased continuously forming TiO₂ nanotube arrays. Figure 1(b) shows the cross section image of TiO₂ nanotube arrays. The thickness of TiO₂ nanotube arrays was 8.55 μm. Figure 1(c) and (d) show the magnified image of Fig. 1(b) and the top surface image of TiO₂ nanotube arrays, respectively. The outer diameter and wall thickness of TiO₂ nanotube arrays were ~125 and ~20 nm, respectively.

Initially formed TiO₂ nanotubes have amorphous phase. Annealing as-anodized TiO₂ nanotubes at 500 °C for 30 min converts amorphous into anatase crystalline phase. Figure 2 shows XRD analysis data of (a) Ti bulk metal, (b) as-anodized TiO₂ nanotubes, and (c) annealed TiO₂ nanotubes. The diffraction patterns of (a) and (b) showed only Ti metal peaks because as-anodized TiO₂ nanotubes have amorphous phase. Annealed TiO₂ nanotube arrays had polycrystalline anatase structures characterized with preferred (101) orientation with (104), (200), (105) and (211) orientations.

Figure 3 shows I–V characteristic curves of the DSCs based on bare TiO₂ nanotubes and MgO coated TiO₂ nanotubes. The short-circuit-current (J_{sc}), open-circuit-voltage (V_{oc}), fill factor (FF) and overall cell efficiency (η) were increased by MgO coating on TiO₂ nanotube arrays, as compared to the sample using bare TiO₂ nanotube arrays. The cell efficiency was decreased, as the concentration of Mg(CH₃COO)₂·4H₂O was increased from 0.02 to 0.04 M in aqueous solution for MgO coating. As summarized in Table 1, photovoltaic performance was highest when the MgO coating concentration was 0.02 M.

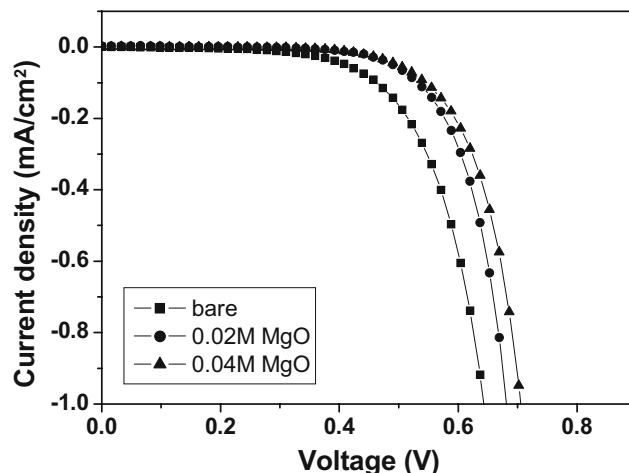


Fig. 4 Dark current measurement for DSCs based on bare TiO₂, 0.02 M MgO coated TiO₂, and 0.04 M MgO coated TiO₂ nanotube arrays

The overall conversion efficiency was increased from 0.16 to 1.61%.

Increased photovoltage was attributed to the reduced charge recombination. MgO coating layer formed an energy barrier between TiO₂ nanotubes and electrolyte. This energy barrier inhibited back transfer of TiO₂ electrons to electrolyte reducing charge recombination. The insulating effect by MgO layers on TiO₂ nanotubes increased the photovoltage. The photocurrent was also increased due to the improvement of dye adsorption. This can be explained by using the isoelectric point (IEP) of MgO and TiO₂. IEP means pH at which an immersed oxide surface has zero net charge. If pI (IEP) of an immersed oxide is lower than pH of the solution, the solid oxide surface has negative charge. If pI of an immersed oxide is higher than pH of the solution, the solid oxide surface has positive charge. The IEPs of TiO₂ and MgO are 6.2 and 12.4, respectively [16]. If pH of an immersing solution is below 6.2 and over pI of dye molecules, the oxide surface has positive charge and dye molecules have negative charge. The MgO surface in an immersing solution is more positive than the TiO₂ surface due to the higher IEP of MgO. This indicates that the attractive force between MgO surface and dye molecules is stronger than that of TiO₂ surface and dye molecules. Additionally, tiny MgO particles created on TiO₂ nanotube surface increase an overall surface area adsorbing dye molecules. Therefore, we can get DSCs having increased amounts of dye adsorption by coating MgO layers on TiO₂ nanotubes. As the MgO coating concentration was increased from 0.02 to 0.04 M, the overall conversion efficiency was decreased. This result indicates that MgO layers formed on TiO₂ nanotubes should have an optimum thickness. When the thickness of MgO layers is over an optimum value, injection of photo-excited electrons into the TiO₂ conduction band is inhibited. Photocurrent, as shown in Table 1, was decreased from 3.732 to 2.738 mA/cm² because thick MgO layer blocked the injection of photo-excited electrons.

Figure 4 shows dark current measurement of DSCs based on bare TiO₂ nanotubes and 0.02 and 0.04 M MgO coated TiO₂ nanotubes. The dark current onset shifted to high potential with MgO coating, and the 0.04 M MgO coated sample produced a smallest dark current at the same potential above 0.6 V. These observations reflect that MgO layers on TiO₂ nanotubes have an insulating effect at the interface of TiO₂ and electrolyte. As the thickness of MgO layers is increased, the charge recombination is reduced between TiO₂ and electrolyte.

While 0.04 M MgO coated sample had a superior property in reducing charge recombination between TiO₂ electrons and electrolyte, 0.02 M MgO coated sample showed best conversion efficiency. The MgO layer on TiO₂ nanotube arrays should be have a moderate thickness for high electron injection yield.

4 Conclusions

The overall conversion efficiency of DSCs using 0.02 M MgO coated TiO₂ nanotubes was 1.61%, 10 times higher than that of DSCs using bare TiO₂ nanotubes. We could confirm the MgO coating effect on TiO₂ nanotube arrays from these results. Photovoltage and photocurrent increased with MgO coating. MgO insulating layers formed an energy barrier at the interface of TiO₂ nanotube arrays and electrolyte. This energy barrier reduced charge recombination between TiO₂ and electrolyte. Dye adsorption was improved due to the basicity of the MgO surface. When the MgO coating concentration increased from 0.02 to 0.04 M, the overall conversion efficiency decreased. This indicates that too thick MgO layers formed on TiO₂ nanotube arrays block the charge injection of photo-excited electrons into the TiO₂ conduction band. Therefore, we should control the MgO concentration to achieve the improved efficiency.

Acknowledgements This work was partially supported by “Regional Technology Innovation Program (grant no. RTI05-01-02)” of the Ministry of Commerce Industry and Energy (MOCIE) and “New Renewable Energy Technology Development Program (2007-N-PV08-P-01)” of Korea Energy Management Corporation.

References

1. B. O'Regan, M. Gratzel, *Nature*. **353**, 737 (1991)
2. C.J. Barbe, F. Arendse, P. Comte, M. Jirousek, F. Lenzmann, V. Shklover, M. Gratzel, *J. Am. Ceram. Soc.* **80**, 3157 (1997)
3. P.E. deJongh, D. Vanmaekelbergh, *Phys. Rev. Lett.* **77**, 3427 (1996)
4. J. van de Lagemaat, N.G. Park, A.J. Frank, *J. Phys. Chem. B.* **104**, 2044 (2000)
5. G.K. Mor, O.K. Varghese, M. Paulose, K. Shankar, C.A. Grimes, *Sol. Energy Mater. Sol. Cells.* **90**, 2011 (2006)
6. K. Zhu, N.R. Neale, A. Miedaner, A.J. Frank, *Nano Lett.* **7**(1), 69 (2007)
7. K. Shankar, G.K. Mor, H.E. Prakasam, S. Yoriya, M. Paulose, O. K. Varghese, C.A. Grimes, *Nanotechnology* **18**, 65707 (2007)
8. A. Kay, M. Gratzel, *Chem. Mater.* **14**, 2930 (2002)
9. H.S. Jung, J.K. Lee, M. Nastasi, S.W. Lee, J.Y. Kim, J.S. Park, K. S. Hong, H. Shin, *Langmuir* **21**, 10332 (2005)
10. Z.S. Wang, M. Yanagida, K. Sayama, H. Sugihara, *Chem. Mater.* **18**, 2912 (2006)
11. F. Fabregat-Santiago, J. Garcia-Canadas, E. Palomares, J.N. Clifford, S.A. Haque, J.R. Durrant, G. Garcia-Belmonte, J. Bisquert, *J. Appl. Phys.* **96**(11), 6903 (2004)
12. S.G. Chen, S. Chappel, Y. Diamant, A. Zaban, *Chem. Mater.* **13**, 4629 (2001)
13. K.M.P. Bandaranayake, M.K.I. Senevirathna, P.M.G.M. Prasad Weligamuwa, K. Tennakone, *Coord. Chem. Rev.* **248**, 1277 (2004)
14. M. Paulose, K. Shankar, S. Yoriya, H.E. Prakasam, O.K. Varghese, G.K. Mor, T.A. Latempa, A. Fitzgerald, C.A. Grimes, *J. Phys. Chem. B.* **110**(33), 16179 (2006)
15. J.M. Macak, L.V. Taveira, H. Tsuchiya, K. Sirotna, J. Macak, P. Schmuki, *J. Electroceram.* **16**, 29 (2006)
16. G.A. Parks, *Chem. Rev.* **65**, 177–198 (1965)